Mineralogy, Geochemistry and Fluid Inclusion Studies of the Arinem Te-Bearing Gold-Silver-Basemetal Deposit, Western Java, Indonesia

E. T. Yuningsih (Hokkaido Univ.) and H. Matsueda (Hokkaido Univ. Museum)

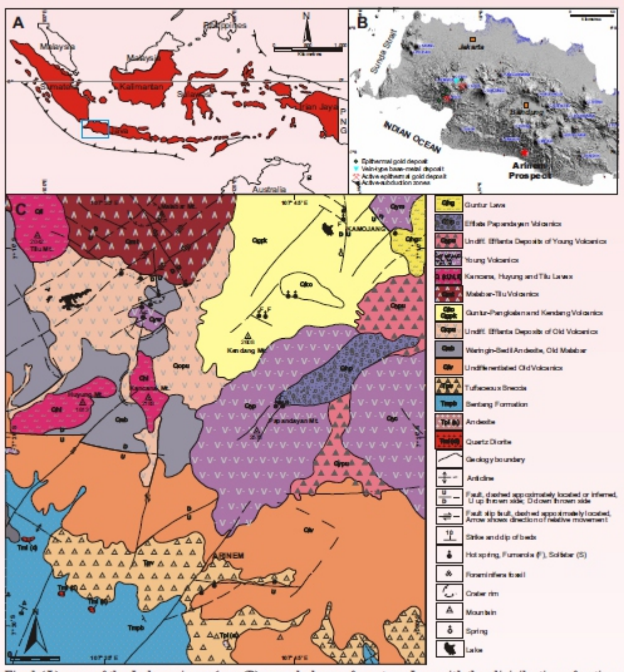

Fig. 1 (A) map of the Indonesia region, (B) morphology of western Java with the disribution of active volcanoes and distribution of gold deposit at western Java. The location of the Arinem prospect is indicated by a red star, (C) regional geological map of the Arinem district and its surroundings (modified after M. Alzwar et al., 1992).

1. Introduction

The Arinem area is located in a part of the Sunda-Banda magmatic arc (well known as gold-copper belt) within the Indonesia archipelago at the southern margin of the Sundaland and the Eurasian plates (Fig. 1A-B). The mineralized body is a quartz vein, trending N140°-160°E and dipping around 68°- 83° for about 5,900m at 3 - 5m width and is exposed at an elevation of 365 - 530m above sea level. Outcrop and drill core samples containing gold and silver are intimately associated with basemetal minerals of copper, lead and zinc.

2. Geological Setting

The ore is hosted in andesitic tuff, breccias, and lava of the Oligocene - Middle Miocene Jampang Formation. The pyroclastic host rocks suffered mainly propylitic and argillic alterations and are characterized by the occurrence of chlorite, sericite, kaolinite, smectite and in place by carbonate as a result of quartz diorite intrusions during Late Oligocene - Middle Miocene. The formation is overlain unconformably by a volcanic group of Pliocene age, which is composed of andesitic breccias and tuff. Later on, this formation was intruded by pyroxene-hornblende andesite of Pliocene age. The youngest lithotypes within the area are volcanic rocks of Pliocene - Pleistocene age (M. Alzwar et al, 1992; Fig. 1C). Four normal faults cut through the research area, the direction is almost North - South. The faults crop out along the Arinem, Bantarhuni and Halimun quartz veins (Fig. 2).

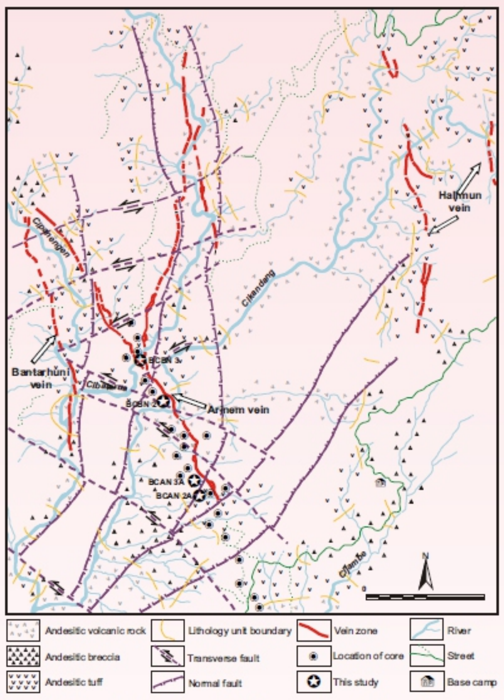

Fig. 2 Geology and structural map of the Arinem vein, western Java, Indonesia. The location of the Bantarhuni and Halimun veins are indicates west and east of the Arinem vein (modified after Antam, 1993).

3. Mineralization and Formation Age

Gold-silver-basemetal vein mineralization from Arinem were classified into three stages (I to III) of quartz-sericite-calcite-sulfide veins which fill fault planes in Oligocene - Miocene volcanic rocks (Fig. 3 and 4). Stages I and II are Au-Ag-bearing, where as stage III is barren (Table 1, Fig. 5, 5a, 5b and 6). K-Ar dating of alteration sericite (8.8±0.3 Ma) indicates a Late Miocene age for the mineralization (Table 2).

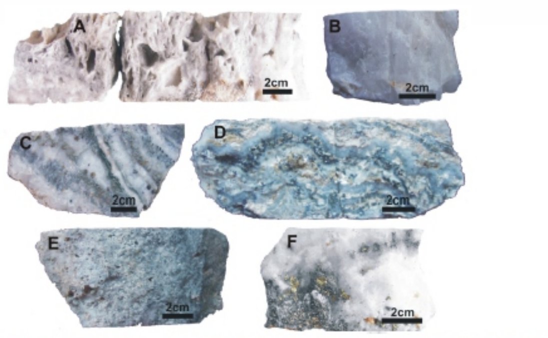

Fig. 3. Hand specimens of Arinem quartz vein from core samples (A) vuggy quartz of stage IA-L-60, (B) barren coarse-grained crystalline quartz of stage IIIB-L275, (C) banded quartz-sulfide of stage IC-L300, (D) banded quartz-sulfide of stage IC-L440, (E) vuggy crystalline quartz of stage IA-L440, (F) crystalline quartz-sulfide of stage IB-L60.

Table 1. Generalized paragenetic sequence of vein minerals in the Arinem deposit. Width of lines correspond to the relative abundance of each mineral

Table 2. K-Ar age of the Arinem vein

Sample No.	Sample description	%K	$^{40}Ar_{rad}$ nl/g	$\%^{40}Ar_{air}$	K/Ar Age (Ma)
BCBN 2-75	Alteration sericite	2.68	0.903	32.4	8.8±0.3

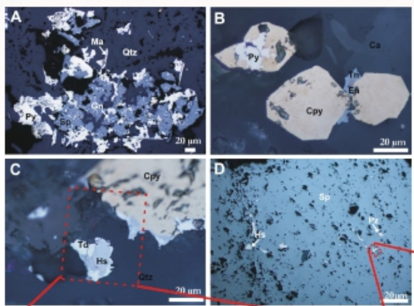

Fig. 5. Reflected light photomicrographs showing the mineralogy and texture of ore minerals from Arinem vein, (A) fine grained galena (Gn) as veinlet in sphalerite (Sp), marcasite (Ma) intergrowth with pyrite (Py) in quartz, sample from substage IB/L440m, (B) pyrite (Py) associated with chalcopyrite (Cpy), enargite (En) replaced by tennantite (Tn) at the margin, ore minerals associated with fine grained calcite and quartz, sample from substage IIC/L265, (C) Te-bearing mineral of hessite (Hs) and tetradymite (Td) as isolated grain and some as inclusion in chalcopyrite (Cpy), sample from substage IIA/L300, (D) sphalerite (Sp) with inclusion of fine grained hessite (Hs) and petzite (Pz), sample from substage IIC/L265. Inset in Fig. 5 (C) and (D) are locations of back scattered electron image mapping (see Figs. 5a and 5b).

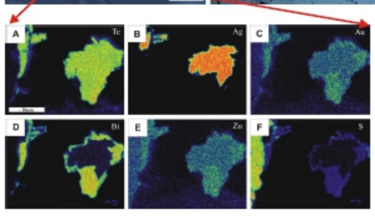

Fig. 5a. A-F characteristic X-ray images of Te, Ag, Au, Bi, Zn and S of tetradymite and hessite minerals. Sample from stage IIA/

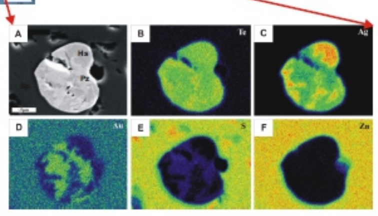

Fig. 5b. (A) back scattered electron image shows the occurrence of hessite (Hs) associated with petzite (Pz) as inclusion in sphalerite (Sp) and its X-ray images characteristics of Te, Ag, Au, S and Zn. Sample from stage IIC/L265m.

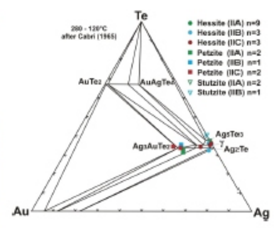

Fig. 6. Chemical composition of hessite, petzite and stutzite from Arinem deposit in comparison with ideal composition of mineral phases plotted on a Au-Ag-Te diagram (Cabri, 1965 in Afifi, 1988).

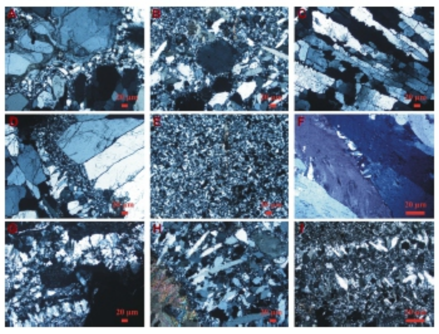

Fig. 4. Photomicrographs showing the occurrence of some quartz textures. (A) botryoidal form of calcedonic texture from outcrop sample, (B) feathered texture of granular quartz with fine- to medium grained quartz/L440m, (C) bladed/lattice texture of quartz pseudomorph after calcite/L440m, (D) fine grained quartz growth at the end of coarse grained quartz/L440m, (E) moss texture of quartz/L300m, (F) feathered re-crystallization texture/L275m, (G) microcrystalline colloform gel banding texture associated with clay and ore minerals/L265m, (H) inherited platy structure in replacement lamellar quartz/L265m, (I) milimeter-scale bands texture of microcrystalline quartz interbanded with fine- to medium-grained quartz/L200m.

4. Fluid Inclusion

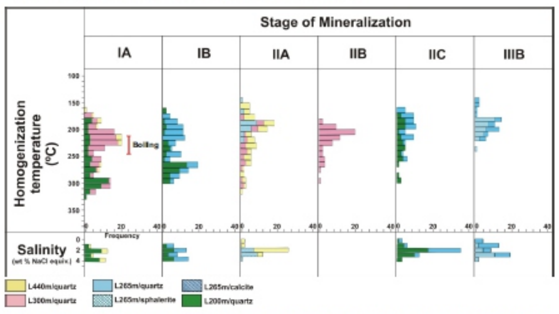

Fig. 7. Range of homogenization temperatures (top) and salinity (bottom) from fluid inclusion in main stage of mineralization (IA - IIC) and barren quartz of stage IIIB showing the slightly decrease of Th from early stage of substage IA to last stage of substage IIIB. Boiling evidence is observed in substage IA with filing temperatures range from 216.8°-

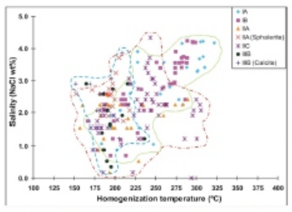

Fig. 8. Homogenization temperature (Th, °C) against salinity (NaCl, wt% equiv.) Plot for fluid inclusion in samples of quartz, sphalerite and calcite from different stages of the mineralized Arinem vein.

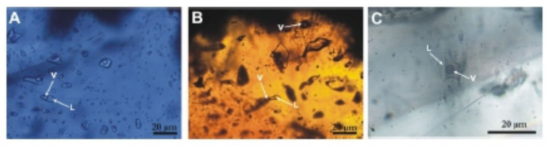

Fig. 9. Photomicrograph of fluid inclusions trapped in quartz, sphalerite and calcite from level 265m of the Arinem quartz vein. (A) group of two phase liquid-rich fluid inclusion as cluster and distributed along the trail in coarse-grain quartz with variable vapor-liquid ratios (vapor bubble occupies up to 40 vol %), (B) two phase liquid-rich primary fluid inclusion coexists with vapor-rich fluid inclusions trapped in sphalerite, (C) isolated two phase liquid-rich primary fluid inclusions trapped in calcite. (transmitted plane-polarized light).

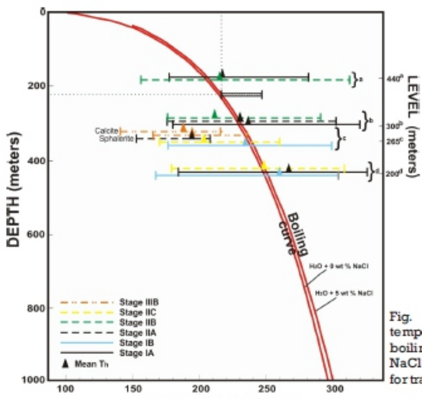

Fig. 10. Range and mean of fluid inclusion homogenization temperatures (Th) versus depth for different substages. Possible boiling point with depth curves for water with 0 wt % and 5 wt % NaCl equiv. (Haas, 1971) are shown. Dashed line showing evidence for trapping of a boiling fluid occurred in substage IA.

5. Geochemistry and Formation Condition

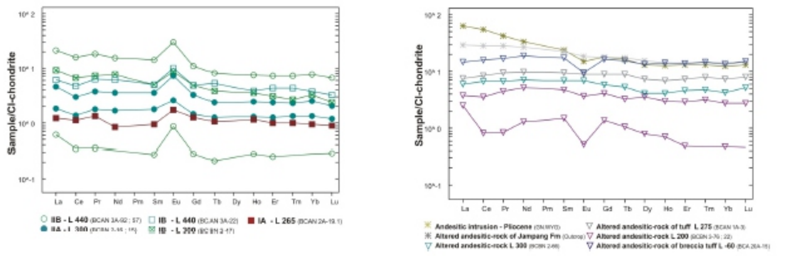

Fig. 11. Chondrite normalized concentration of rare earth elements (La - Lu) of the Arinem quartz vein (left); altered andesitic host rock in comparison with andesitic Pliocene intrusion (right). The REE data were normalized to their abundance in chondrites according to Sun and McDonald (1989).

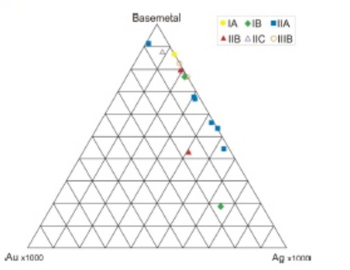

Fig. 12. The representative abundance correlation of Au-Ag-Basemetal (Cu, Pb, Zn) for every stage of Arinem vein.

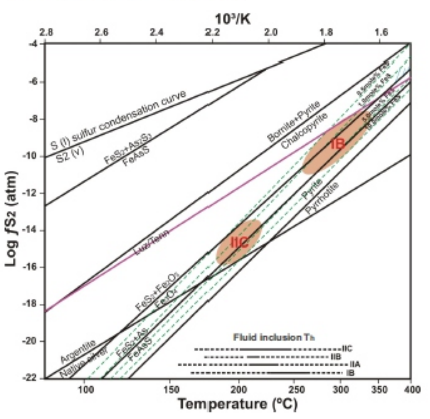

Fig. 13. Sulfur fugacity vs. temperature diagram showing sulfidation reactions of mineral assemblage in the Arinem deposit. Isopleths for sphalerite are calculated from the equations of Scott and Barnes (1971). Shaded areas with red arrow, indicating gold and silver depositional enviroments of stages IB, IIB, C and D show decreasing temperature and sulfur activity with progressing of mineralization stages.

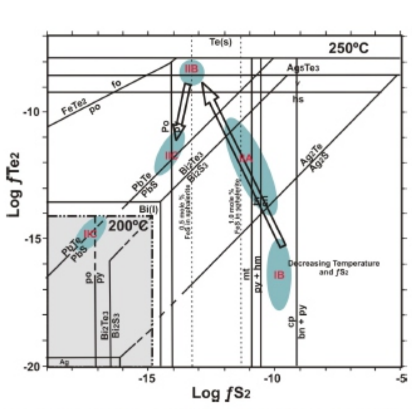

Fig 14. Log fTe_2 vs. log fS_2 diagram indicating equilibria between tellurides and sulfides of Arinem deposit, at 250° and 200°C, at vapor saturation (after Afifi, 1988). Arrows indicate approximate conditions of formation of Te-bearing and sulfide minerals at Arinem deposit.

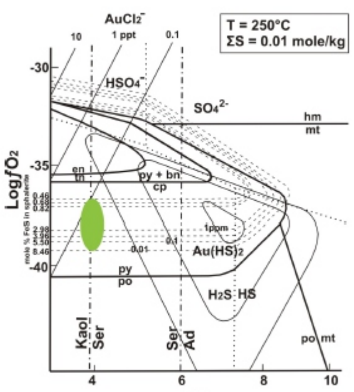

Fig. 15. The possible fO_2 - pH condition of the Arinem ore deposition.

6. Conclusions

The Arinem vein deposit is rich in telluride silver-gold minerals associated with basemetal as indicated by the occurrence of hessite, petzite and stutzite as inclusion in sphalerite, chalcopyrite and galena. No significant ore mineral and compositional variation occurs along the 2000m long and 575m deep Arinem vein suggesting that the hydrothermal system was relatively large. There is no clear linear relationship between fluid inclusion Th and salinity values but boiling evidence is observed in substage IA. Temperature vs. depth profiles for fluid inclusions together with evidence of boiling indicate that the paleo-watertable was located about 235m above the present erosion level during deposition of the main-stage quartz. The ΣREE in mineralized quartz vein is low mostly below 2ppm, with slightly negative Ce and slightly to strongly positive Eu anomalies. Otherwise, samples from altered host rock have ΣREE up to 40ppm and show negative Eu anomaly. The shift in mineralogy reflects a decrease in temperature and sulfur fugacity, with a concomitant increase in fugacity of tellurium during the successive stages of mineralization. The pH-log fO_2 conditions encompass the stability fields of ore fluid at log fO_2 value -39.2 to -36.6, respectively.